Quantized Anomalous Hall Effect in Two-Dimensional Ferromagnets: Quantum Hall Effect in Metals

Masaru Onoda[1,*] and Naoto Nagaosa[1,2,†]

[1]*Correlated Electron Research Center (CERC), National Institute of Advanced Industrial Science and Technology (AIST), Tsukuba Central 4, Tsukuba 305-8562, Japan*

[2]*CREST, Department of Applied Physics, University of Tokyo, Bunkyo-ku, Tokyo 113-8656, Japan*

(Received 23 January 2003; published 22 May 2003)

We study the effect of disorder on the anomalous Hall effect (AHE) in two-dimensional ferromagnets. The topological nature of the AHE leads to the integer quantum Hall effect from a metal, i.e., the quantization of σ_{xy} induced by the localization except for the few extended states carrying Chern numbers. Extensive numerical study on a model reveals that Pruisken's two-parameter scaling theory holds even when the system has no gap with the overlapping multibands and without the uniform magnetic field. Therefore, the condition for the quantized AHE is given only by the Hall conductivity σ_{xy} without the quantum correction, i.e., $|\sigma_{xy}| > e^2/(2h)$.

DOI: 10.1103/PhysRevLett.90.206601 PACS numbers: 72.15.Rn, 73.43.–f, 75.47.–m, 75.70.–i

The origin of the anomalous Hall effect (AHE) has been a subject of extensive controversy for a long term. One is based on the band picture with the spin-orbit interaction [1], while the other is due to the impurity scatterings [2]. Most of the succeeding theories follow the idea that the AHE occurs due to the scattering events modified by the spin-orbit interaction, i.e., the skew scattering or the side jump mechanism [3]. Recently, several authors recognized the topological nature of the AHE discussed in Refs. [4–6]. In this formalism, the Hall conductivity σ_{xy} is given by the Berry phase curvature in the momentum ($\vec{k}$) space integrated over the occupied states [7]. Also, there appeared some experimental evidence supporting it [8]. Therefore, it is very important to study the effect of disorder, which makes $\vec{k}$ ill defined, to see the topological stability of this mechanism for the AHE.

This issue is closely related to the integer quantum Hall effect (IQHE) [9], but there are several essential differences. Usually, the topological stability which guarantees the quantization of some physical quantity, e.g., σ_{xy}, has been discussed in the context of the adiabatic continuation [9]. Therefore, it appears that the gaps between Landau levels in a pure system are needed to start with, even though the disorder potential eventually buries them. In the IQH system without disorder, the periodic potential is irrelevant because the carrier concentration is much smaller than unity per atom. Although numerical simulations [10] use lattice models, the main concern is put on the limit of dispersionless Landau levels separated by the gaps. In the present case, i.e., in ferromagnetic metals, there are multiple bands overlapping without the gaps in the density of states. The periodicity of the lattice remains unchanged, which prohibits the uniform magnetic field and also gives a large energy dispersion. In the language of the effective magnetic field for electrons, it reaches a huge value of the order of $\sim 10^4$ T, i.e., the magnetic cyclotron length is of the order of the lattice constant, but the net flux is zero when averaged over the unit cell. Therefore, these two cases belong to quite different limits although the symmetries of the systems are common, i.e., the unitary class without time-reversal nor spin-rotational symmetry.

In this Letter, we report on an extensive numerical study on two-dimensional (2D) models for the AHE including the disorder potentials. It is found that the topological nature of the AHE leads to a dramatic phenomenon, i.e., the ferromagnetic metal turns into an integer quantized Hall system by introducing disorder. This is due to the topological stability of the Chern numbers carried by the extended states which are energetically separated by the continuum of the localized states in between. Namely, the localized state cannot have a finite Chern number, and the integer topological number cannot change smoothly, i.e., it jumps when it changes. These two facts lead to the protection of the extended state against the weak disorder. The finite-size scaling analysis is compatible with the two-parameter renormalization-group theory of Pruisken [11], which predicts the plateau transition at $|\sigma_{xy}| = 0.5e^2/h$. The critical exponents are consistent with that of the IQHE. This problem is not an academic one; the recent technology can fabricate very fine thin films of ferromagnetic metals with a large enough single domain. When the coherent length of such a thin film is longer than the thickness, it can be regarded as a multichannel 2D system. These systems can offer a possible laboratory to test our theory.

The essence of the AHE is that the Berry phase of the Bloch electron is induced by the spin-orbit interaction in the presence of the magnetization, which is modeled by the complex transfer integrals [5]. Each band often gains a finite Chern number even though the density of states has no gap. The minimal model describing this situation is that proposed by Haldane [12] and its extension. This model is defined on a honeycomb lattice containing two atoms in a unit cell (Fig. 1). Using the Fourier transformation $\boldsymbol{c}^\dagger_{\vec{k}} = (c^\dagger_{A\vec{k}}, c^\dagger_{B\vec{k}})$ of the spinor representation

$(c^\dagger_{\vec{r}\in A}, c^\dagger_{\vec{r}\in B})$, its Hamiltonian is written as $H = \sum_{\vec{k}} \boldsymbol{c}^\dagger_{\vec{k}} \mathcal{H}_{\vec{k}} \boldsymbol{c}_{\vec{k}}$, where

$$\mathcal{H}_{\vec{k}} = 2t_1 \cos\phi \sum_{i=1,2,3} \cos(\vec{k}\cdot\vec{a}^{\rm tr}_i)\tau^0 + t_0 \sum_i [\cos(\vec{k}\cdot\vec{a}^{\rm hc}_i)\tau^1 - \sin(\vec{k}\cdot\vec{a}^{\rm hc}_i)\tau^2] + \left[m + 2t_1 \sin\phi \sum_i \sin(\vec{k}\cdot\vec{a}^{\rm tr}_i) \right]\tau^3. \quad (1)$$

τ^0 is the unit matrix and $\tau^{1,2,3}$ are the Pauli matrices. Here we assume the perfect spin polarization and use the spinless fermions. The complex next-nearest neighbor hopping integral $t_1 e^{i\phi}$ is introduced in addition to the real one t_0 between the nearest neighbors. $\vec{a}^{\rm tr}_{1,2,3}$ are the lattice vectors of the triangle sublattice, while $\vec{a}^{\rm hc}_{1,2,3}$ are those of the honeycomb lattice (Fig. 1).

The extended model is given by adding another layer with the change $t_1 \to -t_1$ to the original single-layer model given above. Furthermore, we introduce the energy difference between the layers by shifting the uniform potential $\pm u$. Then the extended model has the symmetric and gapless density of states in contrast to the original one. In Fig. 2 are shown the density of states and σ_{xy} for the single-layer [Fig. 2(a)] and double-layer [Fig. 2(b)] models, respectively. In the single-layer case, σ_{xy} is quantized to be e^2/h when the Fermi energy lies within the gap, while it is not in the double-layer case where the gap collapses. We chose in Fig. 2 and below the parameter values as $t_1 = 0.2t_0$, $m = 0.4t_0$, and $\phi = \pi/3$ in order to demonstrate the scaling law most clearly. However, once the scaling law is established, we can discuss more realistic cases as will be done later.

Now we introduce the on-site disorder potential to the single-layer model, which is randomly distributed in the range $[-W/2, W/2]$ and study the localization problem in terms of the transfer matrix method [13]. Figure 3(a) shows the dependence of the renormalized localization length $\lambda_M/(2M)$ of a quasi-1D tube with $2M$ sites circumference. The length of a tube is typically $\sim 10^5$ sites and the accuracy of data is within a few percent. We can see that extended states are isolated in energy. They merge with each other at a critical value $6 < W_c < 7$ and disappear, i.e., all states are localized. This behavior is the same as that observed in the ordinary IQH system on a square lattice with external magnetic field [10]. It is noted that the pair annihilation of extended states always occurs between those with the opposite Chern numbers [10]. Actually, two extended states in Fig. 3 originate from lower and upper bands which have opposite Chern numbers, ± 1, respectively.

Next we analyze the data to obtain a characteristic length $\xi(E, W)$ by the scaling hypothesis, $\lambda_M(E, W)/M = f[\xi(E, W)/M]$, where $f(x)$ is a scaling function [14]. As for a localized state, $\xi(E, W)$ is interpreted as its localization length in the thermodynamic limit. Figures 3(c) and 3(d) show $\xi(E, W = 5.0t_0)$ around the lower extended state at $E = E_c$. From this data, the critical exponent ν ($\xi \propto |E - E_c|^{-\nu}$) and E_c are estimated as $\nu = 2.37 \pm 0.05$ and $E_c = (-0.69 \pm 0.01)t_0$. This value is in reasonable agreement with that estimated in the IQH system [15], e.g., $\nu = 2.35 \pm 0.03$ [16].

In Fig. 3(b) the scaling property of σ_{xy} is shown. There are two critical points where there is no size dependence and which separate the two energy regions with the opposite size dependences. σ_{xy} at these critical points takes the value of about $0.5e^2/h$. This is consistent with the analysis in terms of the effective field theory for the IQH system in the weak-localization region [11] and strongly suggests that the critical properties of this transition are the same as those of the plateau transition σ_{xy}:$0 \leftrightarrow 1$. The energy of these critical points coincide with that where the localization length diverges in

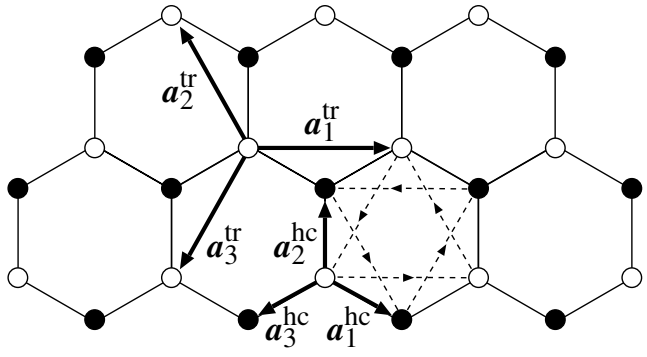

FIG. 1. Haldane's model defined on a honeycomb lattice [12]. Open and solid circles represent the A and B sublattice sites, respectively. The dashed lines represent next-nearest-neighbor hopping.

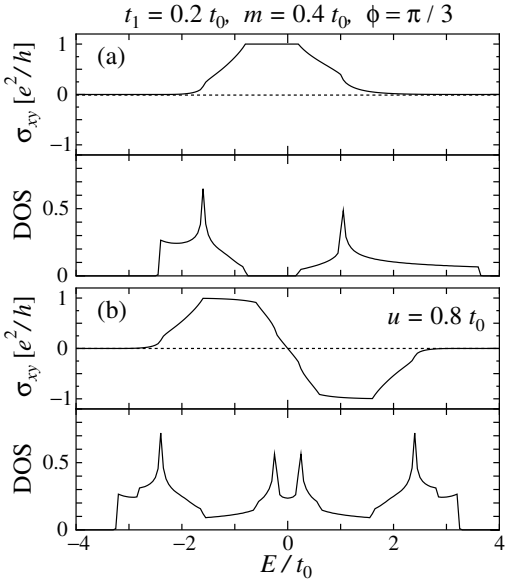

FIG. 2. Hall conductivity σ_{xy} and the density of states for the (a) single-layer and (b) double-layer models.

Figs. 3(a) and 3(c). This means that the extended states with Chern number ± 1 exist there, and σ_{xy} in the thermodynamic limit ($M \to \infty$) stays quantized to be e^2/h between these two energies [broken line in Fig. 3(b)].

Now we consider the double-layer model. The IQHE never occurs in the pure case with the above set of parameters. We consider the case in which there are scattering events both within and between these layers. In this case, there is no gap between the initial and final states of the elastic scattering, and it is possible that all the states are localized once the disorder is introduced. However, as shown below, the extended states and the Chern number carried by them are stable against the weak disorder. Here we define the strength of intralayer scattering as W_0 and represent the strength of interlayer scattering by W_1. As seen in the upper panels in Fig. 4, $\lambda_M/(2M)$ does not show M dependence at $E \cong -1.5t_0$ and $E = 0$. This means that the extended states survive there at least up to $W_1 = 1.0t_0$.

We next present the system-size dependence of σ_{xy} in the lower panels in Fig. 4. There appear two critical points for the transitions σ_{xy}:$0 \leftrightarrow 1$ and σ_{xy}: $-1 \leftrightarrow 1$. From the particle-hole symmetry, $\sigma_{xy}(-E) = -\sigma_{xy}(E)$. Therefore, there appear three critical points in the whole energy region. Because the single-layer model has at most two critical points, the double-layer model could have at maximum four. One may wonder why there appear only three critical points in the present case. This is because the middle one is composed of two extended states which originally contribute to different critical points but carry the same Chern number, i.e., -1. These extended states merge (at least in the present numerical accuracy) but never pair annihilate, because they carry the nonzero Chern number -2. Namely, the conservation law of the topological charge prevents the localization.

σ_{xy} at the lower critical point takes the value $\cong 0.5e^2/h$. This value is again consistent with the analysis in Ref. [11]. However, σ_{xy} at the middle critical point is zero. This critical behavior seems to violate the prediction by the analysis in Ref. [11]. However, recent numerical studies for the IQH system reveal the new type of critical phenomena, i.e., the direct transitions σ_{xy}:$0 \leftrightarrow n$ ($n > 1$) [10], which were experimentally observed in advance [17]. The critical property around the middle point is considered to belong to the same class as σ_{xy}:$0 \leftrightarrow 2$. Although the sample size is not large enough in the double-layer model, the size dependence of σ_{xy} is consistent with the quantized plateau [broken lines in the lower panels of Fig. 4].

It is not difficult to generalize the nonlinear sigma model approach for the localization problem to the case of multicomponent model without time-reversal nor spin-rotational symmetry. These "*components*" mean orbitals,

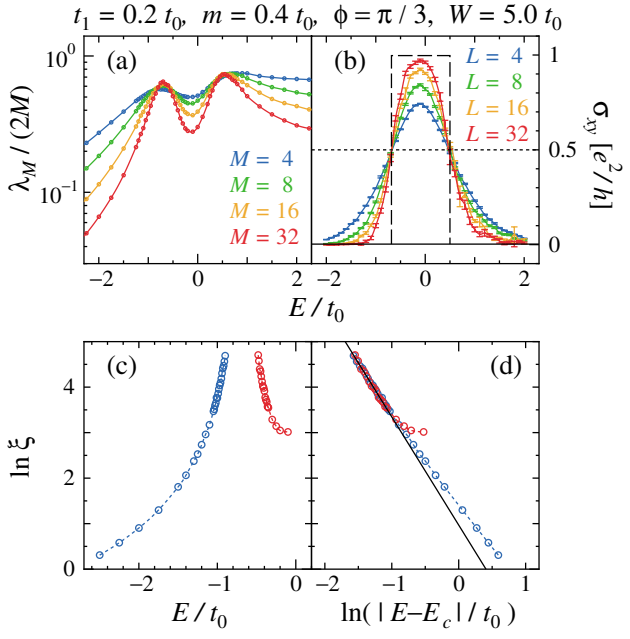

FIG. 3 (color). (a) Localization length λ_M of a quasi-1D tube where M is the number of $A(B)$ sites on the circumference. $M = 4, 8, 16, 32$ are plotted. (b) System-size dependence of σ_{xy} in the single-layer system with $2L \times 2L$ lattice points. The numbers of samples averaged are 81 920, 20 480, 5120, 1280 for $L = 4, 8, 16, 32$, respectively. The errors are one standard deviation. (c) Log plot and (d) log-log plot of localization length ξ around the lower extended state at $E_c = (-0.69 \pm 0.01)t_0$. The solid line is a fitting result with the slope $-\nu = -2.37$. The data of $M = 64$ are included in the analyses for the localization length and its critical exponent.

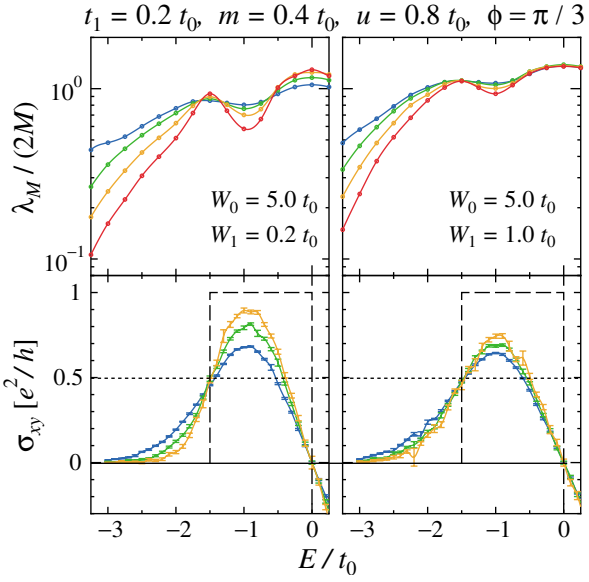

FIG. 4 (color). Upper panels: the localization length λ_M of a quasi-1D tube where M is the number of $A(B)$ sites on the circumference. $M = 4, 8, 16, 32$ are plotted. Lower panels: the system-size dependence of σ_{xy} in the double-layer system with $2L \times 2L$ lattice points. The numbers of samples averaged are 81 920, 20 480, 5120 for $L = 4, 8, 16$, respectively. The color of each line is for the same system size as in Figs. 3(a) and 3(b).

spins, and channels in the multilayer cases altogether. This approach does not assume the finite gap at the start. Following the derivation in Ref. [11], we obtain the Lagrangian

$$L[\{Q_l\}] = -\sum_{l,l'} \frac{1}{2}[g^{-1}]_{ll'} \int d\vec{r} \mathrm{Tr}[Q_l(\vec{r})Q_{l'}(\vec{r})] + \mathrm{Tr}\ln\left[E - \hat{H} + i\eta s + \sum_l iQ_l I_l\right], \quad (2)$$

where $[g]_{ll'}$ is the scattering strength between components l and l', and $[I_l]_{l'l''} = \delta_{l'l}\delta_{l''l}$. Tr (ln) is the trace (logarithm) of a matrix with functional index ($\vec{r}$) and discrete indices (p, a, l), where $p = \pm$ corresponds to the advanced and retarded fields, respectively, and a runs over replicas. The nonlinear sigma model is the effective model for the massless Goldstone modes. In order to extract these modes, the parametrization $Q_l = T_l P_l T_l^{-1}$ is useful. From the above Lagrangian, it is clear that intercomponent scatterings $[g^{-1}]_{ll'}$ ($l \neq l'$) lock the out-of-phase modes $T_l \neq T_{l'}$ ($l \neq l'$), and therefore the effective model for massless in-phase modes, i.e., $T_l = T$, reduces to the model identical to that in Ref. [11]. The coefficients of the stiffness and topological terms for these modes coincide with σ_{xx} and σ_{xy}, respectively. It is noted that these σ_{xx} and σ_{xy} contain the contributions from all components. Then the scaling of σ_{xx} and σ_{xy} remains the same as given in Ref. [11]. This supports the finite-size scaling study given above.

In real systems, the Coulomb interaction cannot be neglected. In the IQH system, the $\ln T$ dependence of σ_{xx} is observed [18] and is attributed to the quantum Coulomb correction [19]. However, the quantized σ_{xy} in the ground state is well described by the noninteracting electron model. The situation is similar here for the quantized AHE. In the thin film of Fe, $\ln T$ dependence of σ_{xx} is observed while not for σ_{xy} [20], which is explained by the quantum Coulomb correction combined with the skew scattering mechanism [21].

Usually the AHE is estimated by $\rho_H \cong -\rho_{xx}^2 \sigma_{xy}$, where ρ_H, ρ_{xx}, and σ_{xy} are measured as quantities in 3D. In good metals, ρ_{xx} is very small at low temperatures, and hence $|\sigma_{xy}|$ is large although $|\rho_H|$ is very small. Therefore, it is possible that the quantized AHE is realized even in the conventional metallic ferromagnets such as Fe or Ni, when the thin film is fabricated. Actually, when we virtually consider thin film of n-layer systems, the 2D $|\sigma_{xy}|$ at $T_C/2$ is estimated as $\sim 0.59ne^2/h$ for Fe [22], $\sim 0.47ne^2/h$ for Ni [22], and $\sim 0.20ne^2/h$ for $SrRuO_3$ (from the first article in Ref. [8]). Therefore, the condition $|\sigma_{xy}| > 0.5e^2/h$ is not so difficult to achieve in the thin films of metallic ferromagnets. Extrapolating the $\ln T$ behavior of σ_{xx} experimentally observed [20], the crossover temperature T_{cross} from weak to strong localization is estimated as $T_{\mathrm{cross}} \cong T_0 e^{-(\sigma_0 h/Ae^2)}$, where T_0 is a reference temperature of the order of 10 K, σ_0 is the Drude conductivity at T_0, and A is a sample-dependent scaling exponent of the order of unity. Therefore, if the minimal $\sigma_0 h/(Ae^2)$ is less than ~ 10, we have the chance to observe the quantized AHE in the experimentally realizable temperature. Considering that σ_{xy} have to be larger than $0.5e^2/h$, this condition means that the ratio σ_0/σ_{xy} should be smaller than ~ 10.

The authors thank Y. Tokura and A. Asamitsu for useful discussion. M. O. acknowledges support by the Domestic Research Fellowship from Japan Society for the Promotion of Science. N. N. is supported by the Ministry of Education, Science, Culture and Sports of Japan.

*Electronic address: m.onoda@aist.go.jp
†Electronic address: nagaosa@appi.t.u-tokyo.ac.jp

[1] R. Karplus and J. M. Luttinger, Phys. Rev. **95**, 1154 (1954); J. M. Luttinger, Phys. Rev. **112**, 739 (1958).
[2] J. Smit, Physica (Amsterdam) **24**, 39 (1958).
[3] J. Kondo, Prog. Theor. Phys. **27**, 772 (1962); P. Nozieres and C. Lewiner, J. Phys. (Paris) **34**, 901 (1973).
[4] J. Ye *et al.*, Phys. Rev. Lett. **83**, 3737 (1999); S. H. Chun *et al.*, Phys. Rev. Lett. **84**, 757 (2000); K. Ohgushi *et al.*, Phys. Rev. B **62**, R6065 (2000); R. Shindou and N. Nagaosa, Phys. Rev. Lett. **87**, 116801 (2001).
[5] M. Onoda and N. Nagaosa, J. Phys. Soc. Jpn. **71**, 19 (2002).
[6] T. Jungwirth *et al.*, Phys. Rev. Lett. **88**, 207208 (2002).
[7] D. J. Thouless *et al.*, Phys. Rev. Lett. **49**, 405 (1982); M. Kohmoto, Ann. Phys. (N.Y.) **160**, 343 (1985).
[8] M. Izumi *et al.*, J. Phys. Soc. Jpn. **66**, 3893 (1997); L. Klein *et al.*, Phys. Rev. B **61**, R7842 (2000); P. Matl *et al.*, Phys. Rev. B **57**, 10 248 (1998); Y. Taguchi *et al.*, Science **291**, 2573 (2001).
[9] *The Quantum Hall Effect*, edited by R. E. Prange and S. M. Girvin (Springer-Verlag, Berlin, 1990).
[10] D. N. Sheng *et al.*, Phys. Rev. B **64**, 165317 (2001); Y. Hatsugai *et al.*, Phys. Rev. Lett. **83**, 2246 (1999).
[11] A. M. M. Pruisken, in *The Quantum Hall Effect* (Ref. [9]), and references therein.
[12] F. D. M. Haldane, Phys. Rev. Lett. **61**, 2015 (1988).
[13] A. MacKinnon and B. Kramer, Z. Phys. B: Condens. Matter **53**, 1 (1983).
[14] E. Abrahams *et al.*, Phys. Rev. Lett. **42**, 673 (1979).
[15] See the review article for the scaling theory of the IQHE, B. Huckenstein, Rev. Mod. Phys. **67**, 357 (1995).
[16] B. Huckenstein, Europhys. Lett. **20**, 451 (1992).
[17] H. W. Jiang *et al.*, Phys. Rev. Lett. **71**, 1439 (1993).
[18] M. A. Paalanen *et al.*, Phys. Rev. B **25**, 5566 (1982).
[19] S. M. Girvin *et al.*, Phys. Rev. B **26**, 1651 (1982).
[20] G. Bergmann and F. Ye, Phys. Rev. Lett. **67**, 735 (1991).
[21] A. Langenfeld and P. Wölfle, Phys. Rev. Lett. **67**, 739 (1991).
[22] J. P. Jan, Helv. Phys. Acta **25**, 677 (1952).